General Disclaimer

One or more of the Following Statements may affect this Document

- This document has been reproduced from the best copy furnished by the organizational source. It is being released in the interest of making available as much information as possible.

- This document may contain data, which exceeds the sheet parameters. It was furnished in this condition by the organizational source and is the best copy available.

- This document may contain tone-on-tone or color graphs, charts and/or pictures, which have been reproduced in black and white.

- This document is paginated as submitted by the original source.

- Portions of this document are not fully legible due to the historical nature of some of the material. However, it is the best reproduction available from the original submission.

SU-SEL-65-010

The Bistatic Radar-Occultation Method for the Study of Planetary Atmospheres

by

G. Fjeldbo and V. R. Eshleman

February 1965

Scientific Report No. 5

Prepared under

National Aeronautics and Space Administration

Research Grant No. NsG-377

RADIOSCIENCE LABORATORY

STANFORD ELECTRONICS LABORATORIES

STANFORD UNIVERSITY · STANFORD, CALIFORNIA

SU-SEL-65-010

THE BISTATIC RADAR-OCCULTATION METHOD FOR THE STUDY OF PLANETARY ATMOSPHERES

by

G. Fjeldbo and V. R. Eshleman

February 1965

Scientific Report no. 5

Prepared under
National Aeronautics and Space Administration
Research Grant no. NsG-377

Radioscience Laboratory
Stanford Electronics Laboratories
Stanford University Stanford, California

THE BISTATIC RADAR-OCCULTATION METHOD FOR THE STUDY OF PLANETARY ATMOSPHERES

N65 18946

Abstract. Theoretical studies have been made of the characteristics of radio waves diffracted at the limb and refracted in the atmosphere of a planet. Sample computations have been made of atmospheric perturbations to the communication links to and from a Mars flyby spacecraft having a trajectory that involves occultation of the spacecraft by the planet as seen from the earth. It is concluded that such a radio occultation experiment can provide important new information on the atmospheric scale height and surface density of a planetary atmosphere, and, when combined with other information, can help determine atmospheric constituents.

Author

Introduction. There already exists a large amount of observational information about the atmospheres on our neighboring planets. The results of the interpretation of these data have been somewhat uncertain, however, mainly because the analyses had to be based on assumptions which are difficult to verify. For this reason various authors arrive at quite different atmospheric models. As an example, let us consider some atmospheric models determined for Mars. Schilling [1962] gives 133 and 41 millibars for the probable upper and lower limits of the atmospheric surface pressure.

Kaplan et al [1964] consider pressures even down to 10 millibars, with an upper limit of 40 mb. From these models the uncertainty in the surface pressure on Mars thus represents a factor of more than 10, and an even larger ratio results from other suggested models. For Mars, the question of the surface density and scale height of the atmosphere has now assumed considerable practical importance because of the desire to land instruments at the earliest possible time (primarily for biological studies), and because the present uncertainties in the atmospheric parameters make it difficult to design such a landing probe.

To be discussed here is a bistatic radar occultation method for the study of planetary atmospheres. It is believed that this experiment can provide more direct information on parameters important to the soft-landing of a spacecraft than has been possible heretofore.

Bistatic radar is differentiated from monostatic radar in that the transmitting and receiving terminals are at different locations in the former. For astronomical applications, we imply that one is on the earth and the other on a space probe. If the trajectory is such that a space probe passes behind a planet as viewed from the earth, the radio ray paths from transmitter to receiver will pass tangentially through the atmosphere and be occulted at the planetary limb. Refraction of the waves in the atmosphere, and diffraction at the limb, can provide a sensitive measure of atmospheric parameters.

The quantity which is fundamental in such an experiment is the profile in height of the refractive index of the atmosphere. Both lower (neutral) and upper (ionized) regions of the atmosphere would in general contribute to this profile. We stress here the determination of the scale height and density of the neutral atmosphere based on the use of only a single radio frequency. A separate publication is being prepared to discuss expected ionospheric characteristics (for Mars, in particular), and the use of a two-frequency occultation technique to afford self-calibration, and to allow the experimental separation of dispersive ionospheric refraction effects from the non-dispersive effects of the neutral atmosphere.

There are a number of different monostatic and bistatic radar techniques not involving occultation which could be used for the study of planetary atmospheres and ionospheres. These would make use of multiple frequency reflections from the planetary surface and from varying depths in the ionosphere. However it appears that the occultation methods would be preferable from the point of view of both simplicity and sensitivity.

A group (A. J. Kliore, F. D. Drake, D. L. Cain, and G. S. Levy) at the Jet Propulsion Laboratory of the California Institute of Technology and the authors have proposed that an experiment such as described here be conducted

using the tracking and telemetry system of the Mariner spacecraft now on its way to Mars. The JPL investigators are particularly concerned with phase and frequency measurements to determine parameters of the neutral atmosphere, and they have made extensive computations of these effects. The Stanford group plans to concentrate on the amplitude and Fresnel diffraction effects caused by the atmosphere, and to study possible ionospheric perturbations to the telemetry signals. All measurements will be made using the facilities of the NASA-JPL Deep Space Network.

General Discussion. The geometry is illustrated in Figure 1. It is assumed that the spacecraft is moving along a trajectory which involves occultation of the spacecraft as viewed from the earth. The communication links or other radio signals to and from the flyby spacecraft can then be used to probe the atmosphere.

The phase and amplitude of the radio waves will vary as the ray paths penetrate the planetary atmosphere. The amplitude changes are produced by focussing and defocussing of the waves, since the amount of refraction imposed by the atmosphere is a function of the depth of penetration of the ray path. It will be shown that continuous measurement of amplitude or phase variations during the occultation may be used to determine the profile in height h of the

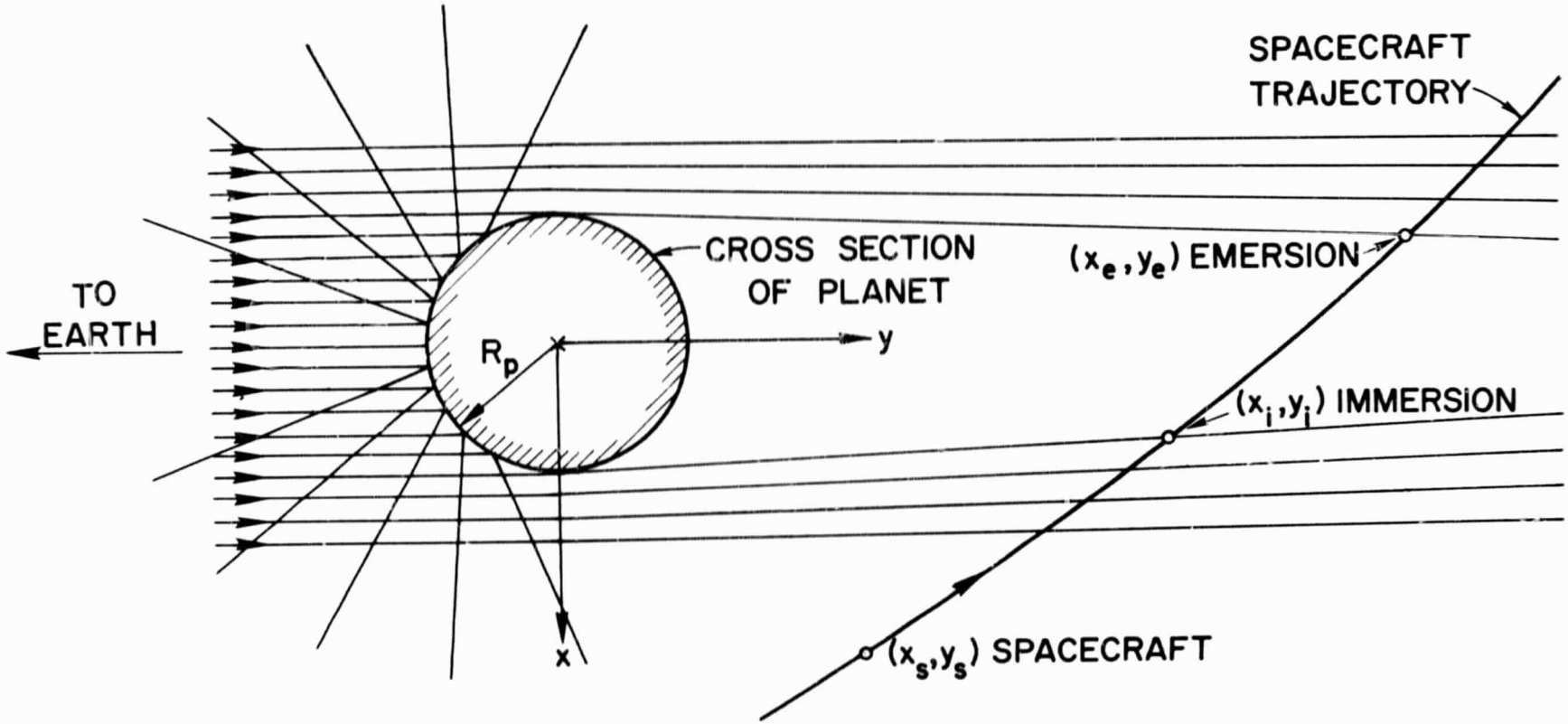

Fig. 1: OCCULTATION GEOMETRY

refractive index μ or the refractivity N in that part of the atmosphere which is probed by the signal. The refractivity and the refractive index profiles are related by

$$N(h) = [\mu(h) - 1] \cdot 10^6 \qquad (1)$$

As a first approximation to the radio phase effect, one can assume straight line propagation through the atmosphere. This simplification gives a first approximation Φ_1 to the phase path increase:

$$\Phi_1(\rho) = \frac{1}{\lambda} \int_{-\infty}^{+\infty} (\mu - 1)\, dy \qquad (2)$$

where λ is the free space wavelength. The geometrical quantities involved are shown in Figure 2. The integral is taken along the straight-line approximation to the ray path. Figure 3 shows how $\Phi_1(\rho)$ may vary as the radius of closest approach for the straight ray path ρ changes during occultation. The first approximation to the phase path increase, obtained by assuming straight-line propagation, is adequate when the spacecraft is close behind the planet.

One can now find the angle α the ray path is refracted. The wave fronts emerging from the atmosphere have been perturbed a distance $[\lambda\Phi_1(\rho)]$ in the y-direction. The corresponding change in the wave normal direction gives:

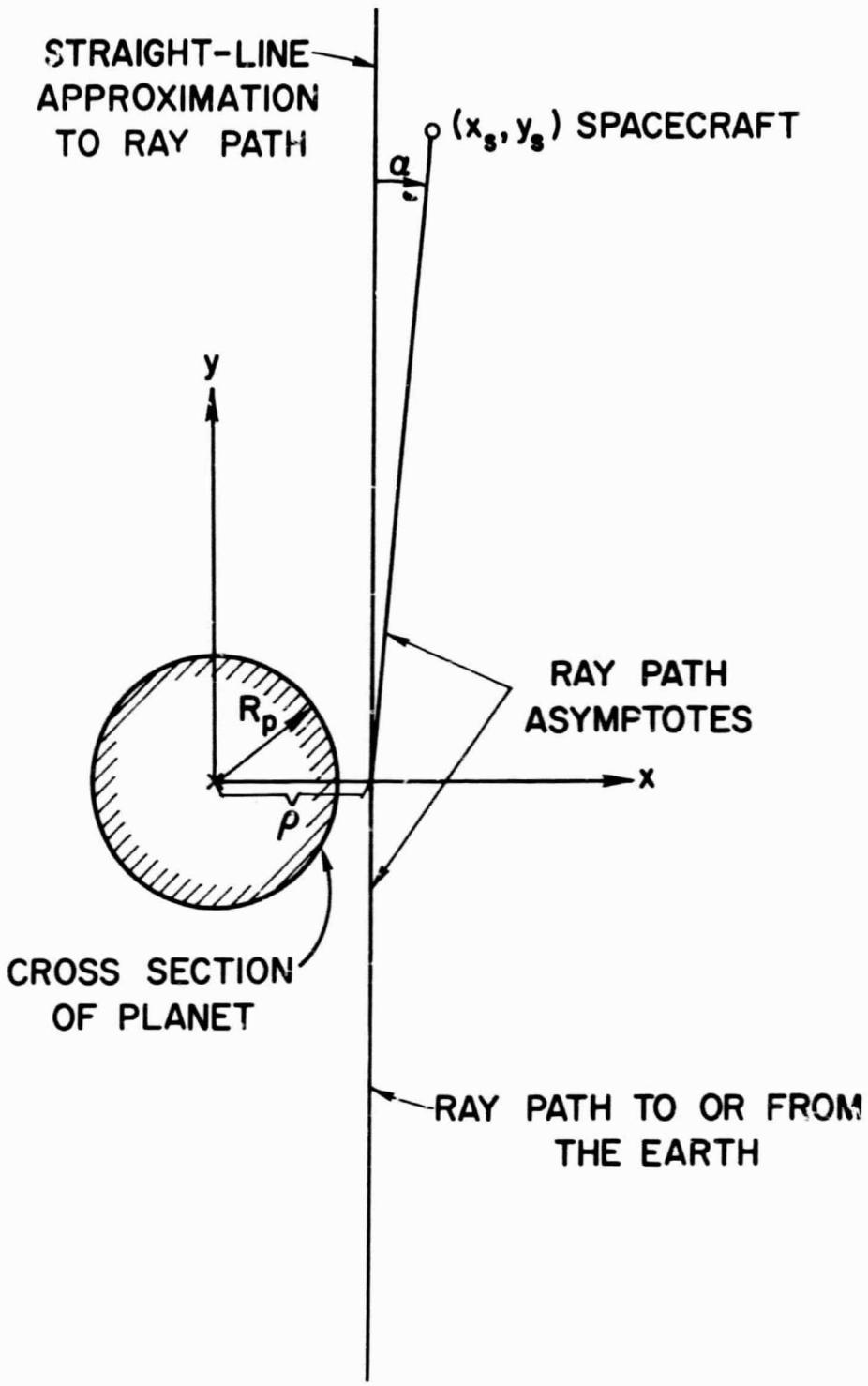

Fig. 2: RAY PATH GEOMETRY

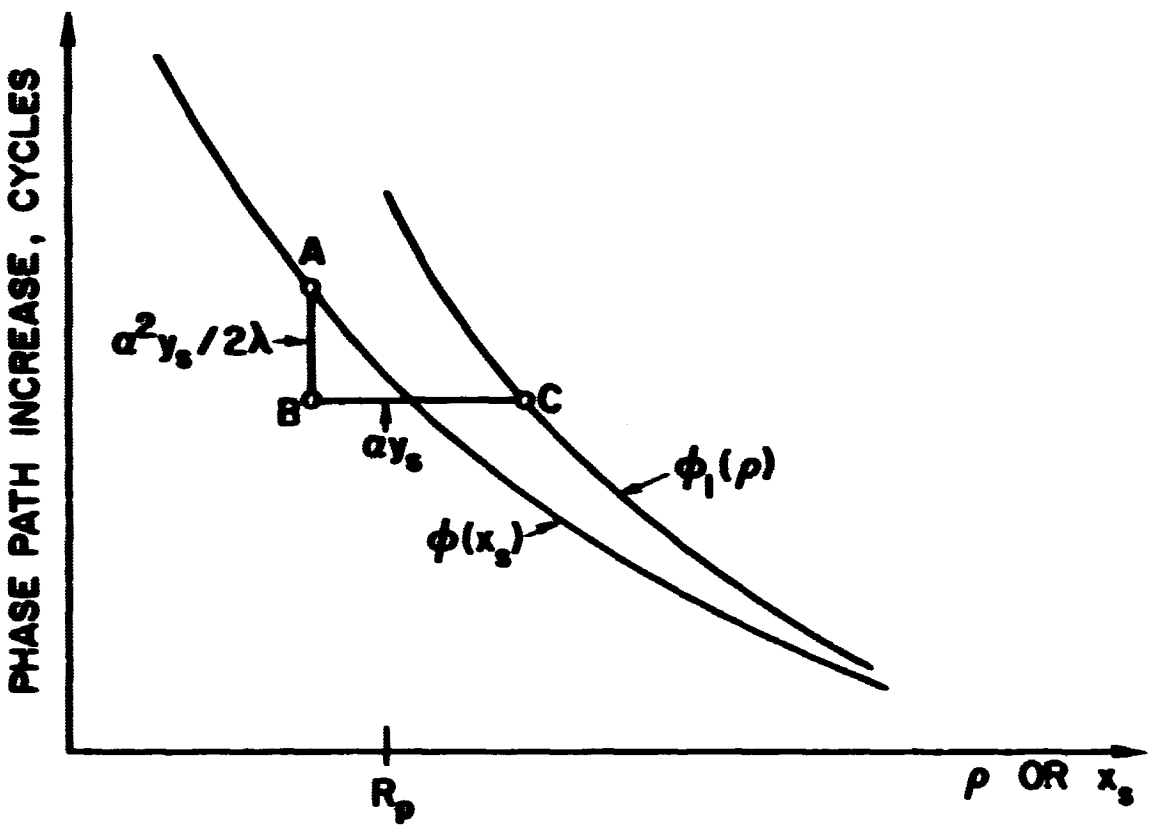

Fig. 3: PHASE PATH INCREASE $[\phi(x_s)]$ AND STRAIGHT-LINE APPROXIMATION TO THE PHASE PATH INCREASE $[\phi_1(\rho)]$

$$\alpha = \lambda \frac{d\phi_1(\rho)}{d\rho} \qquad (3)$$

which is valid for small angles of refraction.

It is important to take into account the bending of the propagation path when the spacecraft is far behind the planet. Approximating the propagation path with two straight line segments along the ray path asymptotes gives the phase path increase ϕ caused by the planetary atmosphere:

$$\phi(x_s) = \phi_1(\rho) + y_s/\lambda \cos\alpha - y_s/\lambda \ .$$

For small α one has

$$\phi(x_s) = \phi_1(\rho) + \alpha^2 y_s/2\lambda \qquad (4)$$

where x_s and y_s are the coordinates of the spacecraft. A phase path measurement yields ϕ for different positions of the spacecraft along the trajectory, and we will therefore consider ϕ a function of the spacecraft abscissa x_s.

The $\phi(x_s)$-curve can be obtained from the construction indicated in Figure 3. By moving from point C on the $\phi_1(\rho)$-curve, a distance αy_s parallel to the abscissa and $\alpha^2 y_s/2\lambda$ cycles parallel to the ordinate gives the corresponding point A on the $\phi(x_s)$-curve.

The refraction in the atmosphere causes focussing of the waves as Figure 1 illustrates. Defining the refraction gain G_r as the change in amplitude due to refraction, one obtains:

$$G_r = -10 \log \left| 1 + y_s \lambda \, d^2\phi_1/d\rho^2 \right| \quad (db) \qquad (5)$$

which is valid when $|\alpha y_s| \ll |x_s|$. The second derivative of $\phi_1(\rho)$ enters into equation (5) because the gain is due to differential refraction.

A more complete derivation of amplitude and phase variations caused by the planetary atmosphere is given by Fjeldbo [1964].

A brief discussion will now be given of how to deduce the refractive index profile from the radio occultation measurements. This process can conveniently be divided into two steps:

1. First, one can determine the straight-line integrated refractive index profile $[\phi_1(\rho)]$ from a measurement of the phase or amplitude variations taking place during the occultation.
2. Second, the refractive index profile $[\mu(\rho)]$ can be calculated from $\phi_1(\rho)$, assuming that the atmosphere may be considered spherically symmetric in those regions probed by the signal.

The first step is easily illustrated by assuming that the phase path curve $[\phi(x_s)]$ in Figure 3 is measured during immersion or emersion. When considering the slope of $\phi(x_s)$ one finds that:

$$\lambda d\phi(x_s)/dx_s = \lambda d[\phi(\rho) + \alpha^2 y_s/2\lambda]/d(\rho + \alpha y_s) = \alpha \tag{6}$$

for small angles of refraction. In other words, $\phi(x_s)$ has the same slope at the point A as $\phi_1(\rho)$ has at the point C. The slope at A, therefore, gives the angle of refraction α. Assuming that the trajectory is known, one can determine the straight-line integrated refractive index $[\phi_1(\rho)]$ by displacing each point on the $\phi(x_s)$ -curve $(\alpha^2 y_s/2\lambda)$ cycles downwards, and a distance (αy_s) parallel to the abscissa axis.

It can also be shown that the amplitude measurements may be used to find the straight-line integrated refractive index $[\phi_1(\rho)]$. This method utilizes equation (5).

The last step consists of calculating the refractive index profile. Equation (2) relates $\mu(\rho)$ to $\phi_1(\rho)$. Solving for $\mu(\rho)$ gives:

$$\mu(\rho) = 1 + (\lambda/\pi) \int_{\xi=\rho}^{\infty} [\phi_1(\rho) - \phi_1(\xi)]\, \xi\, (\xi^2-\rho^2)^{-3/2} d\xi \tag{7}$$

where ξ is a dummy variable of integration.

For numerical integration of equation (7) it is convenient to split the integral into two integrals: one from ρ to $\rho+\Delta\rho$ and one from $\rho+\Delta\rho$ to ∞. The first integral can then be evaluated after expanding the integrand. In this way, one obtains:

$$\mu(\rho) - 1 = -(\lambda/\pi)(\Delta\rho/2\rho)^{1/2} d\Phi_1(\rho)/d\rho + (\lambda/\pi) \cdot \int_{\rho+\Delta\rho}^{\infty} [\Phi_1(\rho) - \Phi_1(\xi)] (\xi^2-\rho^2)^{-3/2} \xi \, d\xi \qquad (8)$$

where $\Delta\rho$ is chosen small enough so that $\Phi_1(\rho)$ can be approximated by its tangent in the interval ρ to $\rho+\Delta\rho$. The advantage of using equation (8) is that the pole of $(\xi^2-\rho^2)^{-3/2}$ is outside the integration interval.

The refractive index profile of the atmosphere is related to the density profiles of the different constituents in the neutral atmosphere and to the electron density profile in the ionosphere. The refractivity of the ionosphere is inversely proportional to the square of the frequency (assuming the radio frequency is much higher than the plasma frequency), while the refractivity of the neutral atmosphere is nearly independent of frequency. Thus one could use a frequency for studying the neutral atmosphere which is so high that the ionospheric effects would be negligible. Even for much lower frequencies, however, a separation in height of the two regions would

make it possible to separate effects of the neutral atmosphere near the surface from higher ionospheric perturbations when the propagation paths passing through the neutral atmosphere are relatively unaffected by the ionosphere except for a constant phase shift. The next section assumes that such a separation is possible.

Application to an Exponential Atmosphere. For a mixed lower atmosphere similar to the earth's, one can approximate the refractivity profile with an exponential function of height:

$$N(h) = N_s \cdot \exp(-h/H). \qquad (9)$$

In this section it will be shown how the perturbations of the probing signal are related to the scale height H and the surface refractivity N_s.

The neutral atmosphere will change the phase path in the manner illustrated in Figure 3. The rate of change in $\Phi(x_s)$ is the Doppler shift of the signal caused by the planetary atmosphere.

Figure 4 shows the phase change for grazing ray propagation. The frequency is set equal to 2300 Mc/s which is the approximate telemetry frequency being used on the 1964-65 flyby mission to Mars. A reduction in the scale height is seen to result in a shorter phase path for low surface refractivity because the total number of neutral molecules along the path is then reduced. However,

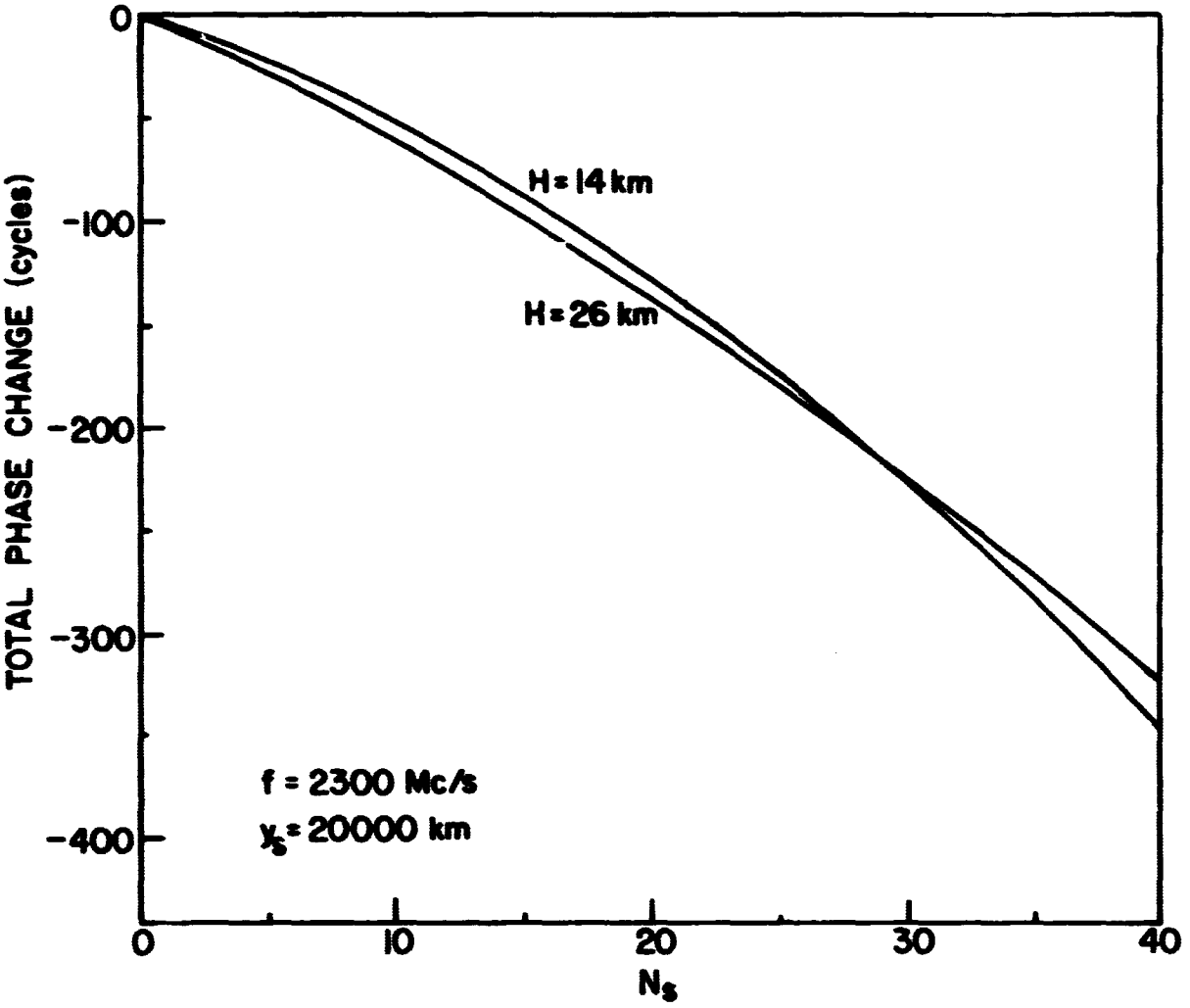

Fig. 4: PHASE CHANGE FOR GRAZING RAY PROPAGATION VS. ATMOSPHERIC SURFACE REFRACTIVITY

for a larger refractivity at the surface, a reduction in the scale height causes larger bending of the propagation path and this more than cancels the effect of reducing the number of molecules along the path. Thus, the curves in Figure 4 cross each other when N_s is increased.

With $N_s = 10$ (which may correspond approximately to a surface pressure of 30 mb), it is seen in Figure 4 that the atmosphere causes a phase path change of about 50 cycles (or 6.5 m) for grazing ray propagation. Figure 5 shows the rate of change in phase path with x_s. The velocity in the x-direction of the Mariner-Mars spacecraft is expected to be about 2 km/sec during the occultation by Mars. With $N_s = 10$ and $H = 26$, this yields an extra Doppler shift of about 4 cps due to the neutral atmosphere. It is seen that high precision measurements and exact computations of spacecraft trajectories will be required to detect the atmospheric perturbations.

The signal amplitude is reduced due to defocussing by the neutral atmosphere as shown in Figure 6. The amplitude variations shown here are strictly correct only for infinite frequency. At other frequencies the amplitude will exhibit Fresnel diffraction oscillations in the vicinity of the shadow boundary. This effect is illustrated in Figure 7 where the stippled curve assumes a smooth horizon and no atmosphere on the planet. With some

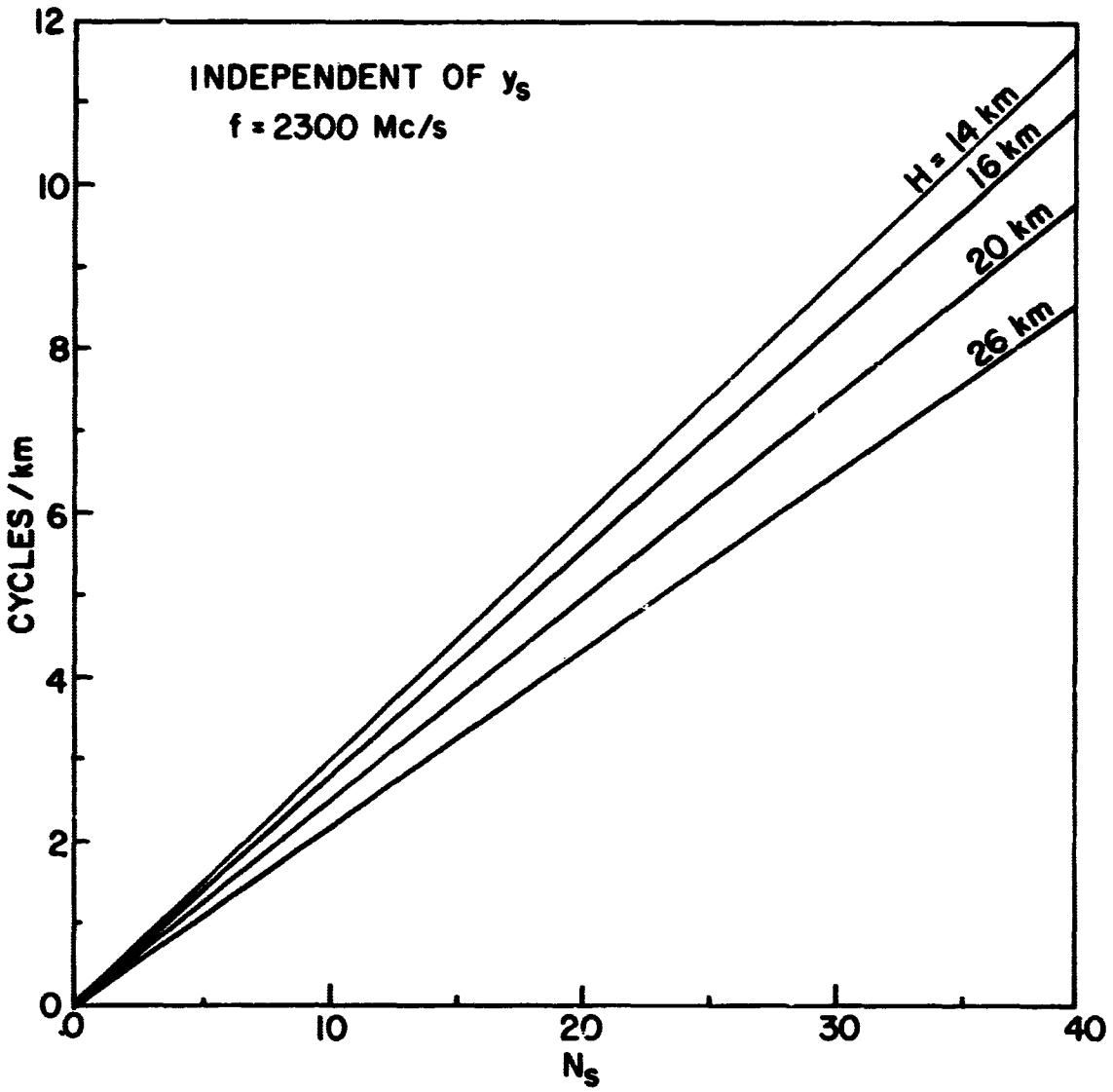

Fig. 5: RATE OF CHANGE IN PHASE PATH VS. ATMOSPHERIC SURFACE REFRACTIVITY

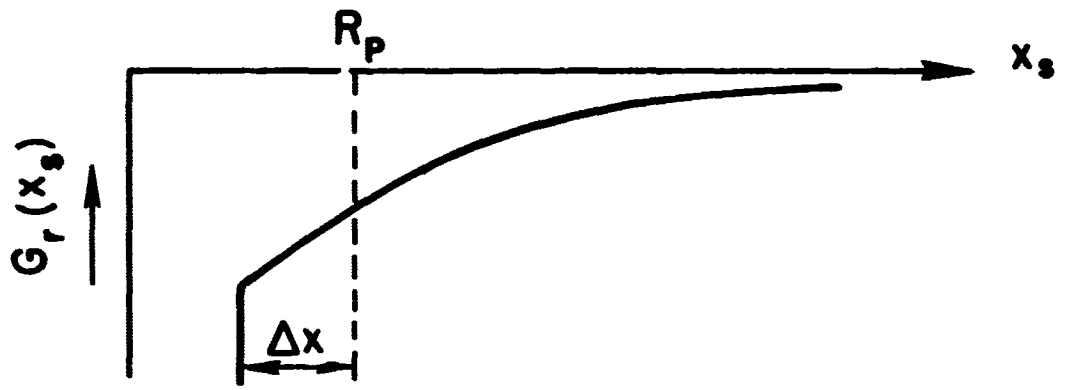

Fig. 6: REFRACTION GAIN VS. SPACECRAFT ABSCISSA

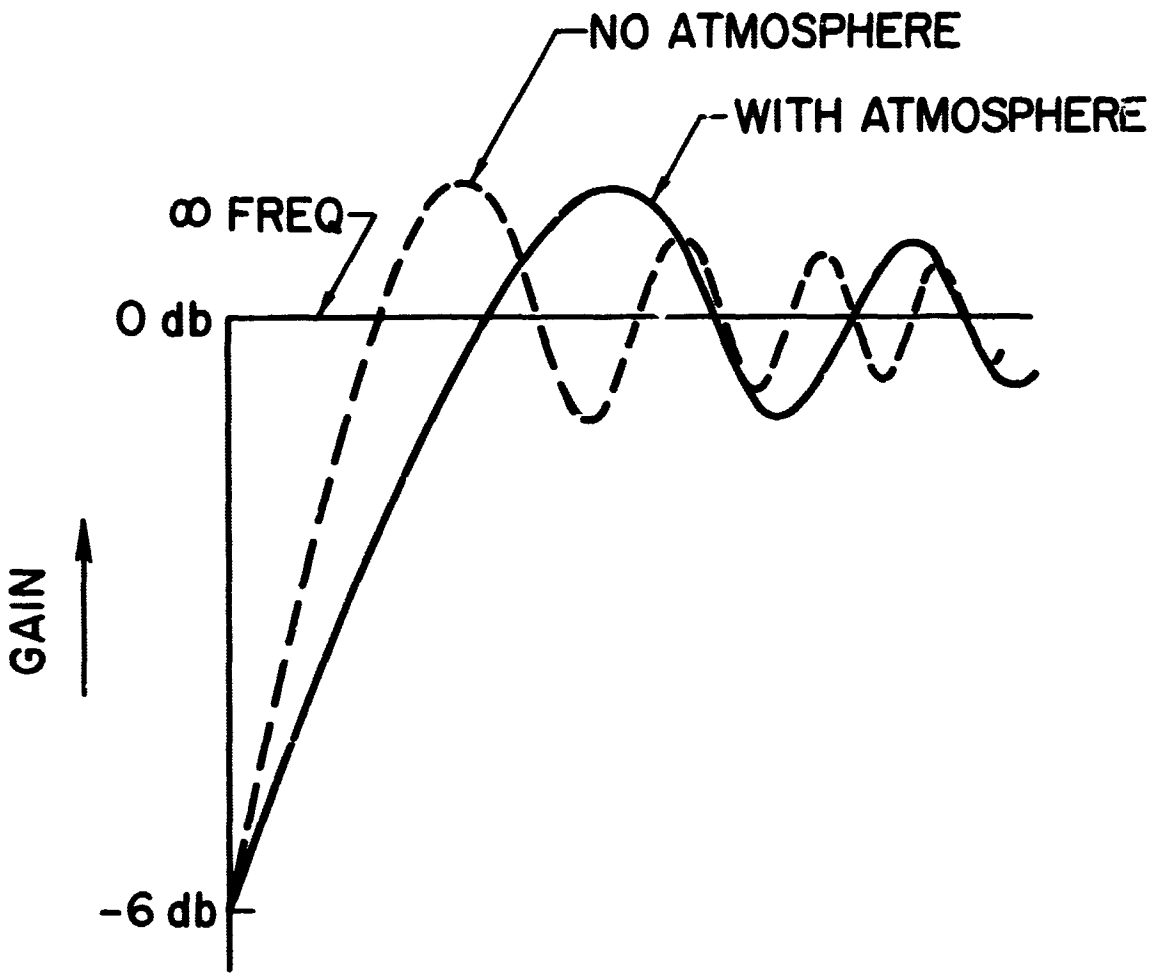

Fig. 7: AMPLITUDE OSCILLATIONS DUE TO DIFFRACTION AT THE PLANETARY LIMB

atmosphere, one gets another diffraction pattern. If the two diffraction curves are drawn through the same -6 db point, one finds that the neutral atmosphere tends to stretch out the diffraction curve (Fresnel stretch).

The refraction gain G_r and the percentage Fresnel stretch for the first diffraction period F are shown in Figures 8 and 9 for grazing ray propagation.

From Figure 6 it is seen that the refraction due to the neutral atmosphere tends to bend the propagation path around the limb of the planet. This grazing ray refraction can be calculated from a measurement of the time that elapses between signal extinction and commencement, assuming that the radius of the planet is known to a sufficient degree of accuracy. Figure 10 shows how much the atmosphere shifts the shadow boundary Δx for different atmospheric models.

For propagation paths grazing the surface, one has for the limiting dependence for a low density atmosphere:
Phase path increase:

$$\Phi = \frac{1}{\lambda} (\mu_s - 1) (2\pi R_p)^{1/2} H^{1/2} \text{ (cycles)} \quad (10)$$

Doppler shift:

$$f = \frac{1}{\lambda} (\mu_s - 1) (2\pi R_p)^{1/2} H^{-1/2} \text{ (cycles/m)} \quad (11)$$

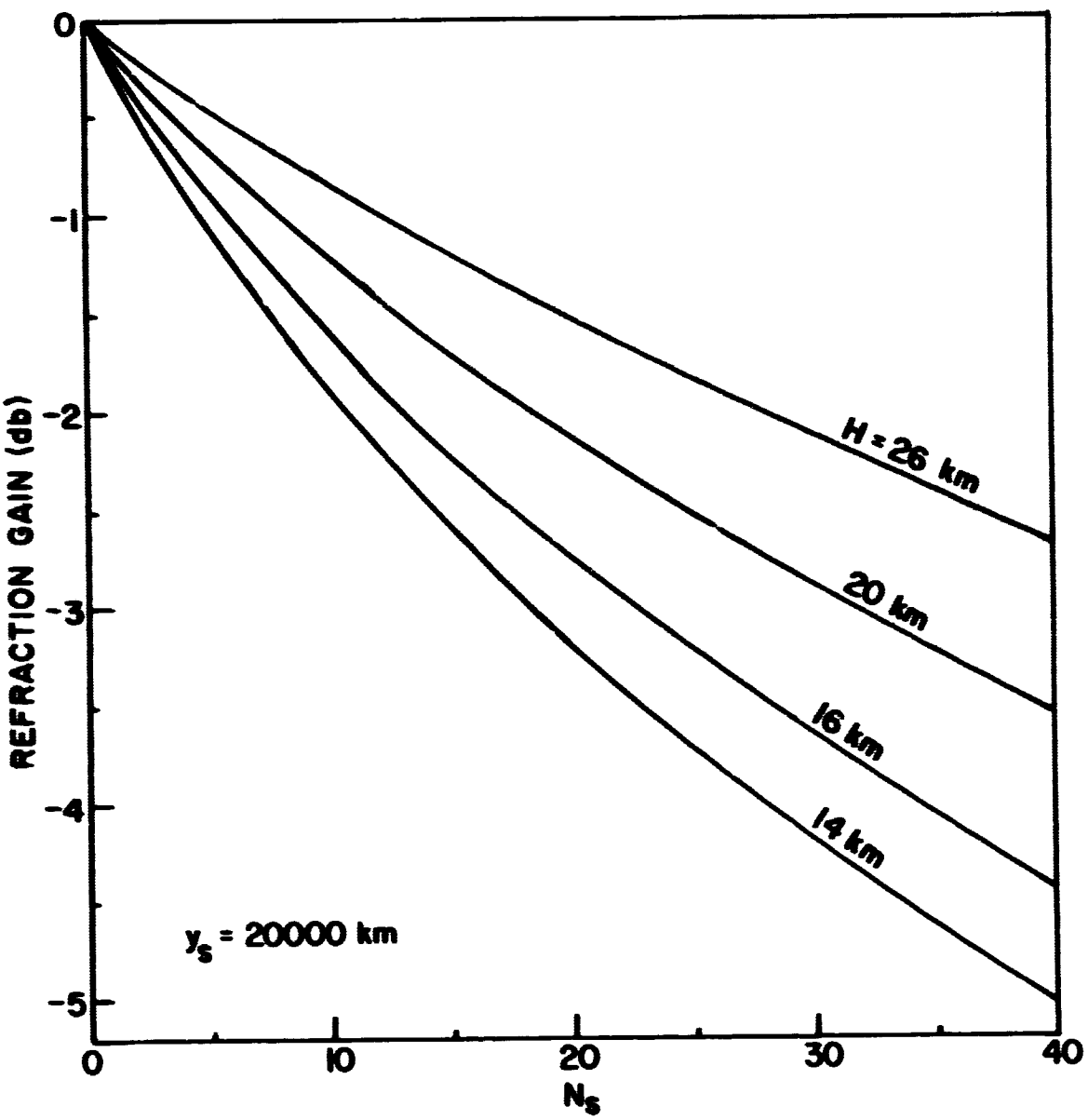

Fig. 8: REFRACTION GAIN FOR GRAZING RAY PROPAGATION VS. ATMOSPHERIC SURFACE REFRACTIVITY

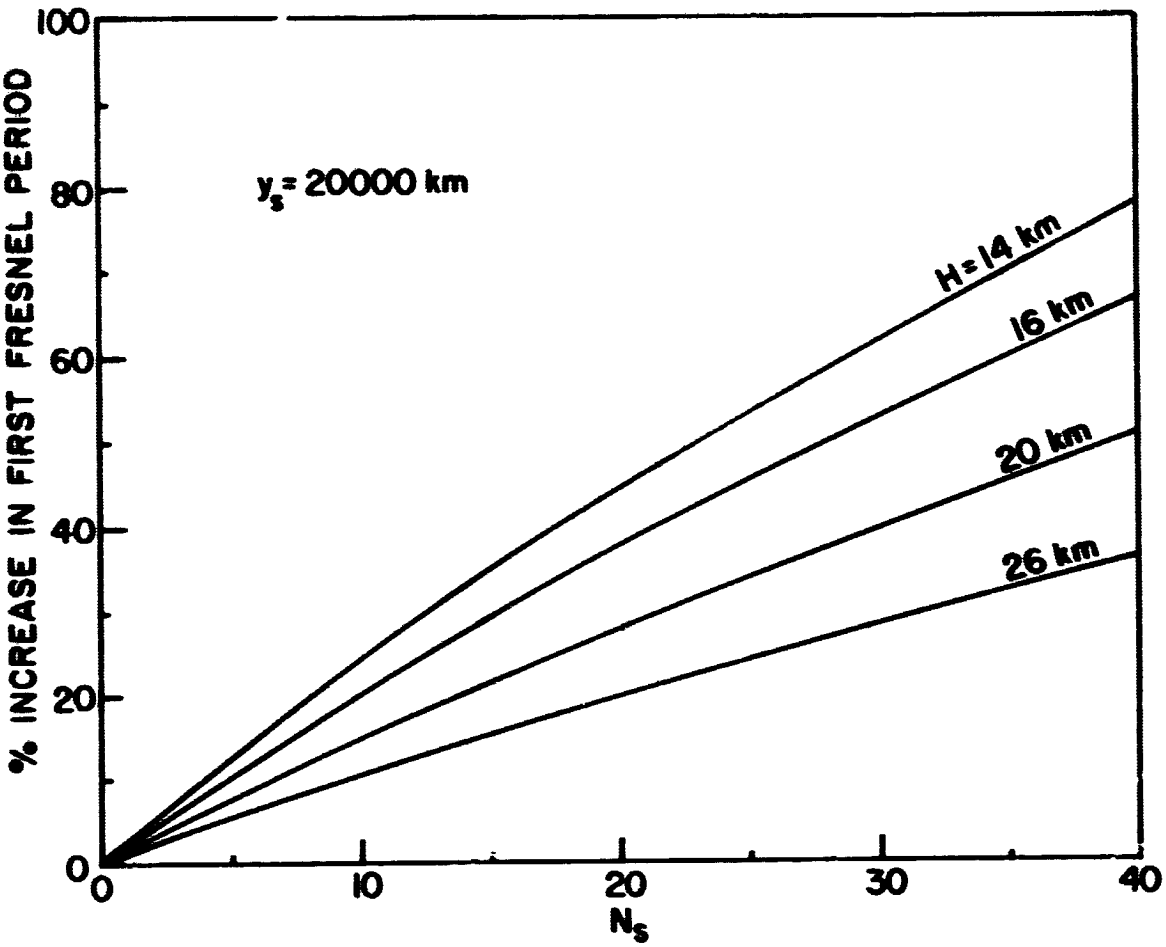

Fig. 9: PERCENT STRETCH OF THE FIRST FRESNEL PERIOD VS. ATMOSPHERIC SURFACE REFRACTIVITY

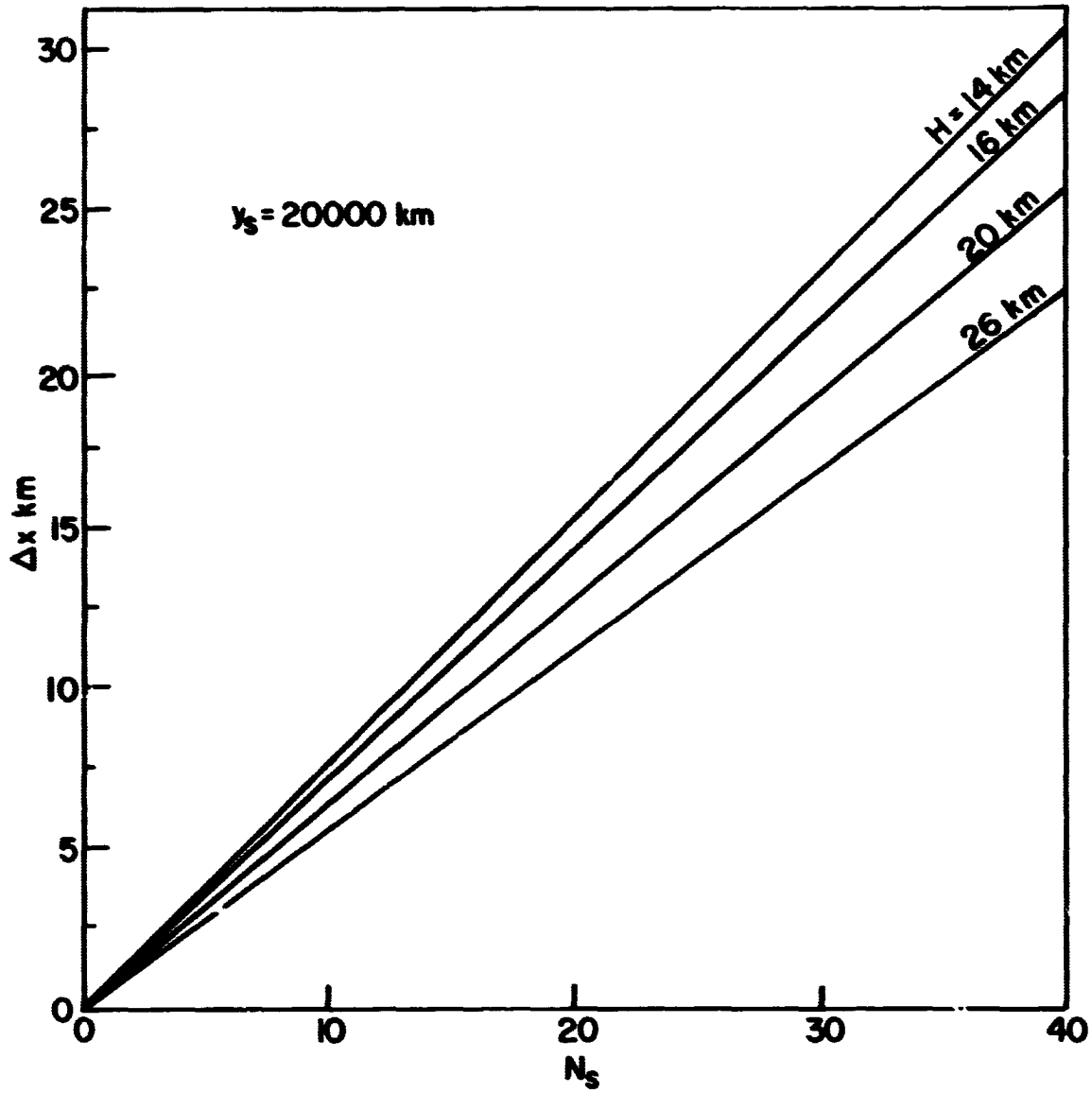

Fig. 10: SHIFT OF THE SHADOW BOUNDARY VS. ATMOSPHERIC SURFACE REFRACTIVITY

Refraction gain:

$$G_r = -4.34(\mu_s - 1)y_s\,(2\pi R_p)^{1/2}\,H^{-3/2} \quad \text{(db)} \qquad (12)$$

Rate of change in G_r:

$$S = -4.34(\mu_s - 1)y_s\,(2\pi R_p)^{1/2}\,H^{-5/2} \quad \text{(db/m)} \qquad (13)$$

Fresnel stretch:

$$F = 50(\mu_s - 1)y_s\,(2\pi R_p)^{1/2}\,H^{-3/2} \quad \text{(percent)} \qquad (14)$$

Refractive displacement of the shadow boundary:

$$\Delta x = (\mu_s - 1)y_s\,(2\pi R_p)^{1/2}\,H^{-1/2} \quad \text{(m)} \qquad (15)$$

where λ denotes the free space wavelength, R_p the radius of the planet, and y_s the distance between the planet and the spacecraft. The refractive index at the surface μ_s is related to the refractivity at the surface N_s by $\mu_s = 1 + N_s \cdot 10^{-6}$. (16)

The quantities Φ, f, G_r, S, F, and Δx are all potentially measurable. Determination of H and N_s requires measurement of at least two of these quantities--for instance G_r and its time rate of change.

Equation (12) does not, by the way, include possible absorption in the planetary atmosphere. However, this absorption may be found from measurement of the gain at both immersion and emersion since the absorption would be independent of y_s while the refraction gain is proportional to y_s.

Measurement of the refraction gain requires that the transmitter power and receiver gain remain constant during the experiment. It may be easier to detect the Fresnel stretch effect from the rapid changes in relative signal amplitude, than to detect a decibel or so of average refraction gain. However, both measurements would yield a value for $(\mu_s - 1)\, H^{-3/2}$.

Equation (14) and Figure 9 assume a smooth horizon in the region where the propagation path is grazing the surface. A more complete analysis reveals that a rough limb tends to wash out the diffraction pattern when the obstacles on the horizon are comparable in size to the first Fresnel zone. However, diffraction patterns similar to those shown in Figure 7 have been observed during radio source occultations by the moon. For instance, Figure 1c in the reference by Hazard et al [1963] shows many distinct diffraction oscillations even though the source, in that case, was an extended weak noise source. One might expect, therefore, to see a large number of diffraction oscillations when a relatively strong coherent point source is occulted by Mars.

Some power will also be reflected from the limb of the planet. Accurate estimates of the reflected signal power cannot be made since little is known about the Martian surface. However, based on calculations assuming

a smooth planetary limb, one finds that the reflected part of the telemetry signal is much too weak to cause any discrimination problems with the trajectory, transmitter power, and receiver gain available for the 1965 occultation. The smooth limb assumption may not be too realistic. However, a rough limb is on the average expected to reflect less power towards the earth than would a smooth limb, because the effective aperture is smaller due to shadowing and because the scattering is no longer coherent. The conclusion therefore remains the same.

The accuracy with which the parameters H and N_s can be determined from amplitude or Fresnel stretch measurements is affected by the planet-spacecraft separation distance y_s at occultation. In general, a short distance and small surface refractivity result in small amplitude or period changes and hence a large uncertainty in the measurement. Very large distances and high refractivity also produce large uncertainties because of the large reduction in signal strength resulting in a low signal-to-noise ratio.

There is a broad minimum with the optimum condition for least uncertainty in the measurement of U per data point being at:

$$Uy_s = 2 \tag{17}$$

where $U = (\mu - 1)\,(2\pi R_p)^{1/2}\,H^{-3/2}$.

For values of Uy_s near 0.5, the uncertainty in the measurement of U increases very rapidly with decreasing values of Uy_s. Using this as a minimum desired value, it follows that:

$$y_{s\ min} = \frac{0.5}{U} \quad . \tag{18}$$

The minimum desired value of y_s is independent of the signal-to-noise ratio prior to occultation although the magnitude of the uncertainty in U for any value of y_s of course decreases with increasing signal strength.

The phase path increase Φ is relatively independent of y_s. Hence, for the phase path measurement it does not make much difference where the trajectory is located as long as the atmosphere is occulted and the signal-to-noise ratio remains high enough to make the measurement possible.

The above analysis applies to a single data point. An increase in y_s tends to spread out the occultation over a greater time, thus enabling more data points to be obtained. This adds emphasis to the importance of having a relatively large planet-spacecraft separation distance.

Estimation of the Atmospheric Surface Density on Mars.

The design of landing probes to perform biological exploration of the surface on Mars requires an accurate knowledge of the physical properties of the lower atmosphere. In particular, the density and scale height must be known fairly accurately in order to design a parachute, and a capsule that can withstand aerodynamic heating and deceleration forces.

The radio occultation experiment yields scale height H and surface refractivity N_s. These quantities are furthermore related to the densities of the different constituents in the lower atmosphere of Mars.

The mean molecular weight m can be determined from the scale height since the temperature T is fairly well known from telescope measurements of radiation from Mars at centimeter and infrared wavelengths. The surface gravity g can be found with good precision from orbital perturbations during the flyby.

The mean molecular weight m provides us with the following relation between the densities n_ν of the different constituents:

$$\sum_{\nu=1}^{M} (m_\nu - m)\, n_\nu = 0 \qquad (19)$$

where m_ν is the molecular weight of the ν-th constituent and M is the number of constituents.

The lower Martian atmosphere is believed to consist mainly of non-polar molecules. Hence:

$$\sum_{\nu=1}^{M} \alpha_\nu n_\nu = N_s \qquad (20)$$

where $\alpha_\nu n_\nu$ is the refractivity of the ν-th constituent. The refractivity has been determined for some of the pertinent gases [Essen and Froome, 1951].

The Martian atmosphere evidently contains CO_2 [Schilling, 1962; Kaplan et al, 1964; and Chamberlain, 1962]. By analogy with the terrestrial atmosphere, one also expects a considerable amount of N_2.

Assuming that N_2 and CO_2 are the main constituents, one can determine n_{N_2} and n_{CO_2} from equations 19 and 20. For instance, if

$$m = 29.6 \pm 10\%$$

$$N_s = 8.44 \pm 10\%$$

have been found from the occultation experiment, one finds that the densities lie within the hatched area in Figure 11. For the total density one obtains:

$$n_{N_2} + n_{CO_2} = 7.2 \times 10^{17}\ cm^{-3} \pm 18\%.$$

The uncertainties in n_{N_2} and n_{CO_2} are larger than 18 percent. Other data may be used to reduce the ambiguities. For instance, Kaplan et al [1964] have analyzed

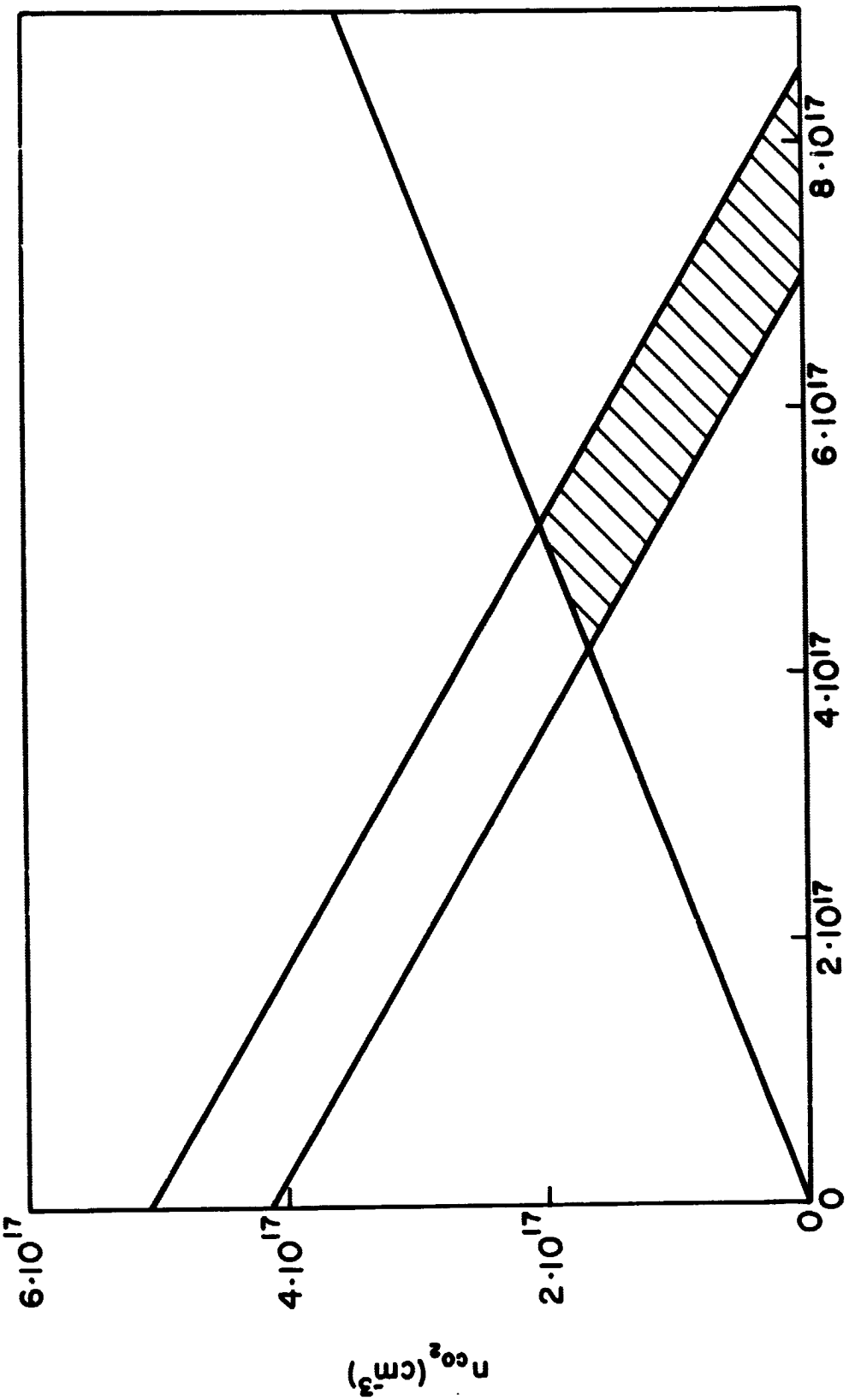

Fig. 11: ESTIMATION OF ATMOSPHERIC DENSITY FROM REFRACTIVITY AND MEAN MOLECULAR WEIGHT AT THE SURFACE

the optical spectrum of Mars and determined the amount of CO_2 along the vertical through the atmosphere. Their results can be utilized to find the density of CO_2 at the surface when the scale height is determined from the radio occultation experiment.

The ionospheric electron density profile can be determined if the refractive index profile for the upper atmosphere has been found from the radio occultation experiment. The electron density profile may also be used to reduce ambiguities in the lower atmosphere since ion recombination rates are quite sensitive to the relative abundance of the different constituents.

Kaplan et al [1964] consider atmospheric models with three main constituents: namely, N_2, CO_2, and A. Equations 19 and 20 can also be used to estimate limits for the densities in this case. The uncertainties in the partial densities, however, get larger with the more constituents the model contains, because one has only two equations. It therefore becomes increasingly important to make use of other data to reduce these ambiguities. However, the total density can still be estimated quite well from equations 17 and 18, especially if the coefficients α_v have nearly the same magnitude as is the case for instance for N_2, A, O_2, and other gases.

The atmospheric density found from the radio occultation experiment would be the density in the region where the propagation path grazes the surface. This region would most likely be at a higher altitude than the mean surface, so that the measured density would be less than the mean atmospheric surface density. But such a bias would be desirable when application is made to the design of an early landing probe, since the probe might land in an elevated region.

Acknowledgment. The research reported here was undertaken as a part of a broad investigation of the potentialities of bistatic radar for space research, under sponsorship of the National Aeronautics and Space Administration. We would like to acknowledge the benefit of discussions with O. K. Garriott, L. A. Manning, and F. L. Smith, III. As indicated above, a Mariner-Mars telemetry occultation experiment was independently suggested by a group at the Jet Propulsion Laboratory for the study of the neutral atmosphere of Mars. Co-experimenters from JPL and Stanford will be involved in the current 1964-5 Mariner mission.

REFERENCES

Chamberlain, J. W., Astrophys. J., 136, 582-593, 1962.

Essen, L. and K. D. Froome, Proc. Phys. Soc. London, B, 64, 862-875, 1951.

Fjeldbo, G., Final Report, NSF G-21543, SU-SEL-64-025, Stanford Electronics Laboratories, Stanford University, Stanford, California, April 1964.

Hazard, C., M. B. Mackey, and A. J. Shimmins, Nature, 197, 1037-1039, 1963.

Kaplan, L. D., G. Munch, and H. Spinrad, Astrophys. J., 139, 1-15, 1964.

Schilling, G. F., J. Geophys. Res., 67, 1170-1172, 1962.